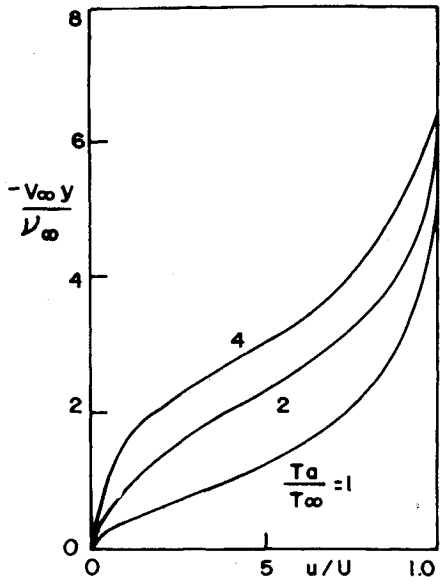


Fig. 1 Velocity profiles at the center symmetric plane.

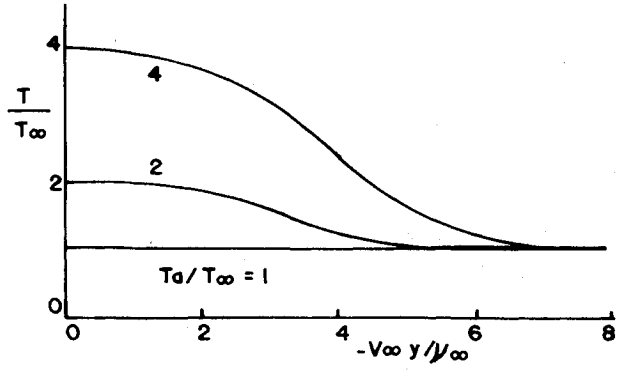


Fig. 2 Temperature profiles at the center symmetric plane.

where $Pr$ is the Prandtl number, $T_u = dT/du$, and $T_{uu} = d^2T/du^2$. When $Pr = 1$, we have

$$T_{uu} = -(1/C_p) \tag{9}$$

which is the same form as that for two-dimensional flow. Integrating Eq. (9) twice and with the aid of Eq. (5), we have the temperature distribution

$$\frac{T}{T_\infty} = 1 + \left(\frac{T_a}{T_\infty} - 1\right)\left(1 - \frac{u^2}{U^2}\right) \tag{10}$$

Again, it is the same form as that for incompressible flow.

The velocity profile cannot be plotted easily in terms of real coordinates $y$ and $z$, because both $y_1$ and $z_1$ depend on the temperature and the temperature depends on the velocity. Also, an explicit expression cannot be obtained as in the case of two-dimensional flow. Thus, the profiles were obtained by the iteration approach. The incompressible velocity profile is used as the initial profile to calculate the temperature. Then, the new velocity is calculated in terms of the real coordinates. Figure 1 shows the velocity profile at the center symmetric plane for the values of $T_a/T_\infty$. Figure 2 shows the temperature distribution. The incompressible case is also shown. It can be observed that there is a thickening of the velocity and temperature boundary layer with increase of velocity, which agrees with the two-dimensional case.

## References

[1] Schlichting, H., *Boundary Layer Theory*, 6th ed., McGraw-Hill Book Co., New York, 1968, pp. 314-316 and 369-382.

[2] Liu, C. Y., "Asymptotic Suction Flow near a Corner," *AIAA Journal*, Vol. 19, Dec. 1981, pp. 1606-1607.

[3] Maddaus, A. D. and Shanebrook, J. R., "The Three-Dimensional Laminar Asymptotic Boundary Layer with Suction," *Journal of Engineering Mathematics*, Vol. 17, Feb. 1983, pp. 73-91.

[4] Young, A. D., "Note on the Velocity and Temperature Distribution Attained with Suction on a Flat Plate of Infinite Extent in Compressible Flow," *Quarterly Journal of Mechanical and Applied Mathematics*, Vol. 1, Jan. 1948, pp. 70-75.

[5] Liu, C. Y. and Ismail, K.A.R., "Asymptotic Solution of Free Convection near a Corner of Two Vertical Porous Plates Embedded in Porous Medium," *Letters on Heat and Mass Transfer*, Vol. 7, Nov.-Dec. 1980, pp. 457-463.

# Nonreflecting Boundary Conditions for the Complete Unsteady Transonic Small-Disturbance Equation

Woodrow Whitlow Jr.* and David A. Seidel*
*NASA Langley Research Center, Hampton, Virginia*

## Introduction

ONE of the most widely used programs for transonic unsteady aerodynamic analysis is the LTRAN2 code of Ballhaus and Goorjian.[1] That code is used to solve the low-frequency, transonic small-disturbance (TSD) equation

$$A\phi_{xt} = B\phi_{xx} + \phi_{yy} \tag{1}$$

where $\phi$ is a disturbance velocity potential normalized by $cU\delta^{2/3}$, $c$ the airfoil chord, $\delta$ the airfoil thickness ratio, and $U$ the freestream speed. The coefficient $A = 2kM_\infty^2/\delta^{2/3}$, where for an oscillation frequency $\omega$, $k = \omega c/U$, and $M_\infty$ is the freestream Mach number. The coefficient

$$B = \frac{1 - M_\infty^2}{\delta^{2/3}} - M_\infty^2(\gamma + 1)\phi_x$$

where $\gamma$ is the ratio of specific heats. The spatial coordinates $x$ and $y$ and time $t$ are normalized by $c$, $c/\delta^{1/3}$, and $\omega^{-1}$, respectively. Steady-state boundary conditions are used at the airfoil, in the wake, and in the far field.

Houwink and van der Vooren[2] improved LTRAN2 by adding unsteady terms to the airfoil and wake boundary conditions; the resulting code is LTRAN2-NLR. Hessenius and Goorjian[3] added a time derivative term to the downstream condition, as well as unsteady airfoil and wake conditions. Their code, LTRAN2-HI, has been validated in the transonic range by a series of comparisons with experimental data.

The steady-state far-field conditions cause disturbances incident on the computational boundaries to be reflected back into the computational domain. As a result, in LTRAN2 and its variations, the boundaries are placed far enough in the far field such that reflected disturbances do not reach the airfoil

Received May 19, 1983; revision received Feb. 28, 1984. This paper is declared a work of the U.S. Government and therefore is in the public domain.

*Aerospace Engineer, Unsteady Aerodynamics Branch, Loads and Aeroelasticity Division. Member AIAA.

during the computations and cause errors in the calculated solutions. In 1980, Kwak[4] incorporated the nonreflecting boundary conditions of Engquist and Majda[5] into LTRAN2. That allowed a reduction in the physical extent of the computational grid and resulted in a savings of 10-24% in the computer time required to complete a calculation.

Since LTRAN2 is limited to the analysis of airfoils undergoing low-frequency motions, a program XTRAN2L,[6] which is used to solve the complete TSD equation

$$C\phi_{tt} + A\phi_{xt} = B\phi_{xx} + \phi_{yy} \tag{2}$$

($C = k^2 M_\infty^2 / \delta^{2/3}$), has been developed at the NASA Langley Research Center. The XTRAN2L code is a modification of LTRAN2-NLR. Solutions of Eq. (2) are obtained using the alternating-direction-implicit scheme of Rizzetta and Chin.[7] However, the boundary conditions of Ref. 5 are not compatible with Eq. (2). In this Note, nonreflecting far-field boundary conditions that are consistent with the complete TSD equation are presented, along with some representative results that show their effectiveness.

## Determination of the Boundary Conditions

Assuming $B$ to be locally constant, the transformations

$$\xi = x/\sqrt{B}$$

$$\tau = (A/BD)x + (2/D)t$$

where $D = \sqrt{4C + A^2/B}$, were used to transform Eq. (2) into the wave equation

$$\phi_{\tau\tau} = \phi_{\xi\xi} + \phi_{yy} \tag{3}$$

A nonreflecting far-field condition for Eq. (3) is[8]

$$\phi_\tau + \phi_r + \phi/2r = 0 \tag{4}$$

with $r^2 = \xi^2 + y^2$. In untransformed coordinates, Eq. (4) becomes

$$\frac{1}{2}\left(-\frac{A}{B}\frac{x}{r} + D\right)\phi_t + \frac{x}{r}\phi_x + \frac{y}{r}\phi_y + \frac{\phi}{2r} = 0 \tag{5}$$

Allowing $x$ to approach $-\infty$ in Eq. (5) with $y$ finite, the following first-order plane wave condition at the upstream boundary is obtained:

$$\frac{1}{2}\left(\frac{A}{B} + \frac{D}{\sqrt{B}}\right)\phi_t - \phi_x = 0 \tag{6}$$

Similarly, letting $x \to +\infty$ with $y$ finite results in the downstream condition

$$\frac{1}{2}\left(-\frac{A}{B} + \frac{D}{\sqrt{B}}\right)\phi_t + \phi_x = 0 \tag{7}$$

At the top and bottom boundaries, $y \to \pm\infty$ with $x$ finite and Eq. (5) becomes

$$(D/2)\phi_t \pm \phi_y = 0 \tag{8}$$

where + and − represent the top and bottom boundaries, respectively. The function $\phi = f(r - \tau)$ is a solution of Eq. (3) which represents the outgoing waves. Using that solution to replace $\phi_t$ by $-(2B/D)\left[(x/r) - (A/D)\right]^{-1}\phi_x$ (as in Ref. 4), Eq. (8) becomes

$$(BD/A)\phi_x \pm \phi_y = 0 \tag{9}$$

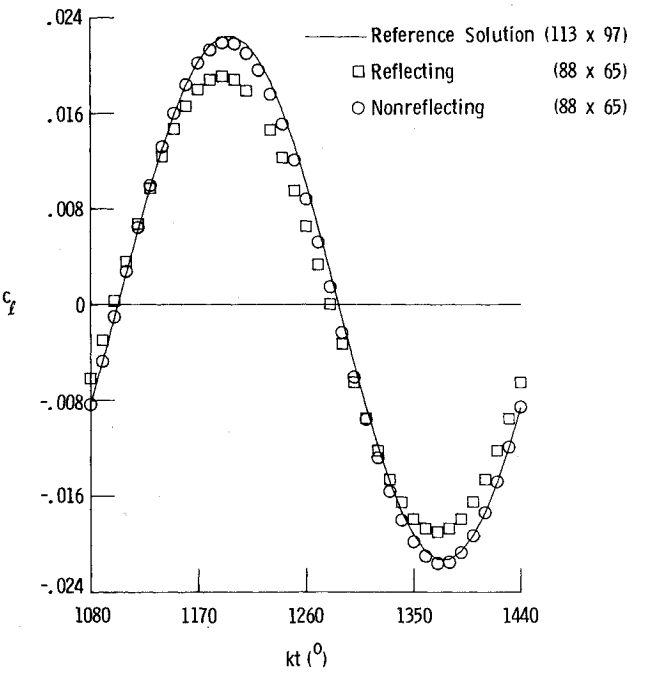


**Fig. 1 Unsteady lift coefficient for an NACA 64A010 ($M_\infty = 0.825$, $k = 0.5$).**

When $C = 0$, Eqs. (6-9) reduce to those presented in Ref. 4 for the low-frequency equation.

## Results

One test of the boundary conditions was to calculate unsteady forces on an NACA 64A010 airfoil pitching harmonically (about its quarter chord) $\pm 0.25$ deg about a 0 deg mean angle of attack at $M_\infty = 0.825$ and $k = 0.5$. A reference solution was calculated for four cycles of oscillation (360 steps/cycle) on a $113 \times 97$ grid (in $x,y$) that extended $\pm 200$ chords (c) in $x$ (the streamwise direction) and 709 c in $y$. The grid was reduced to $88 \times 65$ ($-3.8c \le x \le 3.5c$, $|y| \le 9.3c$) and the calculations were repeated with and without the nonreflecting boundary conditions. The lift coefficients $c_\ell$ for the last cycle of oscillation are shown in Fig. 1. When the steady-state far-field conditions were used on the small grid, disturbances reflected from the boundaries caused the calculated lift to deviate significantly from the large-grid value. After the nonreflecting boundary conditions were implemented, most of the disturbances incident on the boundaries were absorbed and the small-grid results showed good agreement with the reference calculations. Compared with the time required to generate the large-grid solution (3215 s on a CDC CYBER 173), using Eqs. (6), (7), and (9) on the small grid resulted in a 44% savings in computer time. (The small-grid solution with nonreflecting boundary conditions required 1815 s.)

Another test of the boundary conditions was to calculate the unsteady force response for a flat-plate airfoil with a pulse change in angle of attack. The calculations were made for $M_\infty = 0.85$ on an $80 \times 61$ grid that extended $\pm 20c$ in $x$ and $\pm 25c$ in $y$. Using the pulse/transfer function technique described in Ref. 9, the frequency response function for the unsteady lift curve slope $c_{\ell_\alpha}$ was obtained first with steady-state conditions implemented on the boundaries and then with nonreflecting conditions at the boundaries. A flat plate airfoil was used to allow comparisons of the forces calculated using XTRAN2L with those predicted using the exact kernel function method of Bland.[10] Figure 2a shows such a comparison when reflecting boundary conditions were used in XTRAN2L. Below $k \approx 0.5$, the finite difference results had

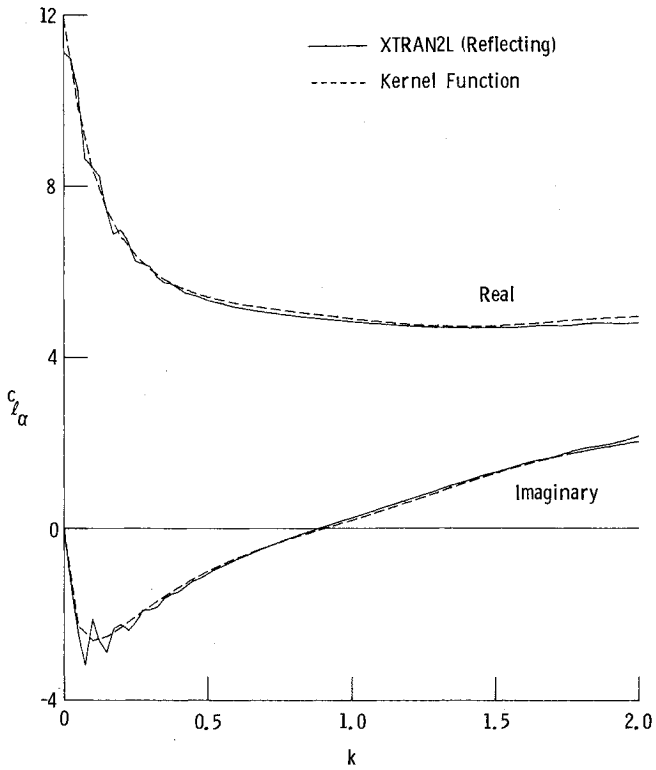


**Fig. 2a Force response for flat plate ($M_\infty = 0.85$, reflecting boundary conditions used in XTRAN2L).**

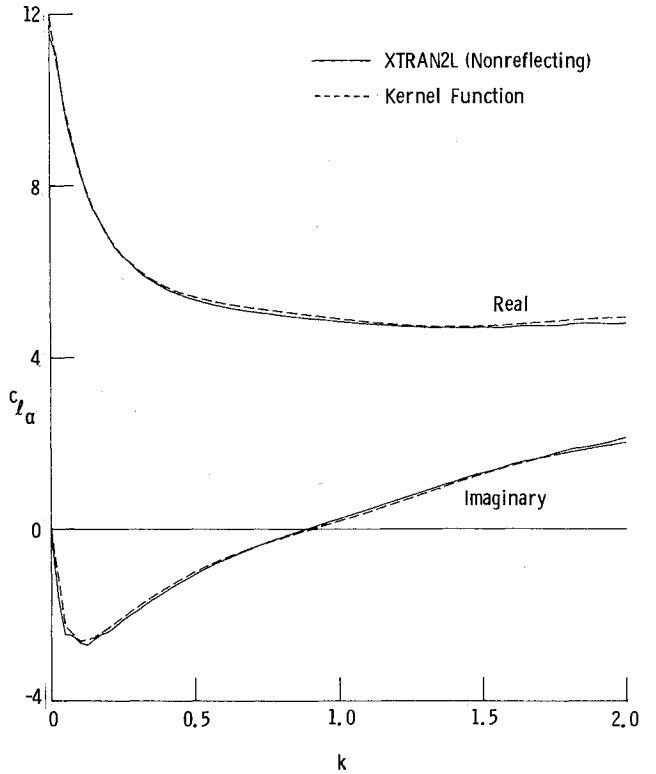


**Fig. 2b Force response for flat plate ($M_\infty = 0.85$, nonreflecting boundary conditions used in XTRAN2L).**

spurious oscillations due to reflected disturbances from the boundaries. When the nonreflecting boundary conditions were used (Fig. 2b), the reflected disturbances were small and good agreement with the exact solution was obtained.

## Conclusions

Nonreflecting far-field boundary conditions that are consistent with the complete transonic small-disturbance (TSD) equation have been derived. They were implemented in a new code for solving the complete TSD equation and were tested for a harmonically oscillating NACA 64A010 airfoil in transonic flow and for a flat-plate airfoil with a pulse in the angle of attack. Using the new boundary conditions on a relatively small grid, solutions for an NACA 64A010 airfoil that agreed with the large-grid calculations were obtained with a 44% savings in computer time. Frequency responses for the flat plate showed that most of the disturbances incident on the computational boundaries were absorbed by the boundary conditions.

## References

[1] Ballhaus, W. F. and Goorjian, P. M., "Implicit Finite-Difference Computations of Unsteady Transonic Flows about Airfoils," *AIAA Journal,* Vol. 15, Dec. 1977, pp. 1728-1735.

[2] Houwink, R. and van der Vooren, J., "Improved Version of LTRAN2 for Unsteady Transonic Flow Computations," *AIAA Journal,* Vol. 18, Aug. 1980, pp. 1008-1010.

[3] Hessenius, K. A. and Goorjian, P. M., "Validation of LTRAN2-HI by Comparison with Unsteady Transonic Experiment," *AIAA Journal,* Vol. 20, May 1982, pp. 731-732.

[4] Kwak, D., "Nonreflecting Far-Field Boundary Conditions for Unsteady Transonic Flow Computation," *AIAA Journal,* Vol. 19, Nov. 1981, pp. 1401-1407.

[5] Engquist, B. and Majda, A., "Numerical Radiation Boundary Conditions for Unsteady Transonic Flow," *Journal of Computational Physics,* Vol. 40, March 1981, pp. 91-103.

[6] Whitlow, W. Jr., "XTRAN2L: A Program for Solving the General-Frequency Unsteady Transonic Small Disturbance Equation," NASA TM 85723, Nov. 1983.

[7] Rizzetta, D. P. and Chin, W. C., "Effect of Frequency in Unsteady Transonic Flow," *AIAA Journal,* Vol. 17, July 1979, pp. 779-781.

[8] Bayliss, A. and Turkel, E., "Far Field Boundary Conditions for Compressible Flows," NASA CP-2201, 1982, pp. 1-19.

[9] Seidel, D. A., Bennett, R. M., and Whitlow, W. Jr., "An Exploratory Study of Finite Difference Grids for Transonic Unsteady Aerodynamics," AIAA Paper 83-0503, Jan. 1983.

[10] Bland, S. R., "Development of Low-Frequency Kernel-Function Aerodynamics for Comparison with Time-Dependent Finite-Difference Methods," NASA TM 83283, May 1982.

# A New Self-Adaptive Grid Method

J.B. Greenberg*
*Technion—Israel Institute of Technology, Haifa, Israel*

## Introduction

THE numerical solution of fluid flow and/or heat and mass transfer problems often entails the necessity to place a high concentration of finite difference points in regions of large gradients, in order to obtain adequate resolution of relevant parameters. In particular, there are many transient situations in which it is desirable to permit the difference grid

Presented as Paper 83-1934 at the AIAA 6th Computational Fluid Dynamics Conference, Danvers, Mass., July 13-15, 1983; received Aug. 5, 1983; revision submitted Dec. 27, 1983.

*Senior Lecturer, Department of Aeronautical Engineering, currently on sabbatical leave at Division of Applied Sciences, Harvard University, Cambridge, Mass.